HEAT AND WATER-VAPOR FLUXES IN AIR FLOWING SOUTHWARD OVER THE WESTERN NORTH ATLANTIC OCEAN[1]

Andrew F. Bunker

Woods Hole Oceanographic Institution

(Original manuscript received 15 April 1959; revised manuscript received 18 September 1959)

ABSTRACT

Turbulent transports of sensible heat and water vapor have been measured from an airplane within southerly-flowing air masses over the western North Atlantic Ocean. It is found that the lower levels of these air masses are unstable and warmed by the transport of heat from the water below, while the higher levels are stable and warmed by diffusion from the subsidence-inversion air aloft. Average values of the upward flux of sensible heat were found to be 2.1 mcal cm^{-2} sec^{-1} in the middle latitudes and 0.1 mcal cm^{-2} sec^{-1} in the tropics. The downward heat flux was 0.3 mcal cm^{-2} sec^{-1} in the region above the potential temperature minimum formed between the warm air aloft and the water-warmed air below. The flux of latent heat of condensation in the form of water vapor was found to be less than the flux of sensible heat from the ocean in the middle latitudes within 300 km of the east coast and about one order of magnitude greater than the sensible flux farther offshore and in the tropics. The observations are discussed in relation to various theories of heat transport and the process by which the atmosphere accumulates heat from the earth's surface.

1. Introduction

The low-level air masses flowing southeastward over the ocean from the polar regions and the trade-wind air flowing southwestward in the tropics have been selected for study as prime examples of relatively cool dry air masses important in the heat-accumulating phase of the atmospheric-heat cycle. As these subsiding diverging air masses flow over the warmer water, sensible and latent heat is transported by turbulent convection into the unstable lower layers. Some of this heat is retained in the subcloud layer, while part of it is transported to higher levels by cumulus-cloud-convection processes. By the time the air masses begin to converge and to ascend in the mid-latitude storms, the equatorial belt, or heated regions of the continents, they are warmer and moister. Part of the water is condensed, releasing the latent heat of condensation, but that which is not condensed in the lifting process is carried throughout the troposphere and indirectly modifies the potential-temperature distribution through the radiative balance. Only the accumulation of heat from the earth's surface is studied in the present paper. The following phase of the heat cycle has been studied by Riehl and Malkus (1958) in their work on the release of energy and the heat balance in the equatorial trough.

To date, the heat and water-vapor flow has been deduced indirectly from accumulations of heat and water vapor, precipitation, estimates of radiational losses, and empirical formulae by Jacobs (1942, 1943, 1951), Riehl *et al.* (1951), Budyko (1956), London (1957), and others. While these methods are invaluable in the determination of the net heating on a global scale, they supply no information about the details of processes operating within the air mass or the magnitude or directions of the heat flows at different heights.

Direct observations of the vertical heat and water-vapor flux are now possible through the development of a system of measuring vertical velocities of the turbulent air from an airplane. This method has been described by Bunker (1955) and Lettau and Davidson (1957). When a record of airplane accelerations, airspeeds, altitudes, dry- and wet-bulb temperatures is reduced, a time series of the values of the turbulent vertical velocities of the air, temperature deviations, and water-vapor deviations is obtained. Values of the flows of sensible and latent heat may be found by averaging the products of the velocities with the temperature and water-vapor deviations.

Flux data of this type have been obtained in selected air masses chosen on the basis of certain characteristics—namely, low-level instability, subsidence, and southerly motion over the western North Atlantic Ocean. One hundred and twenty-five observations have been made at altitudes ranging from 8 m to 2100 m and in latitudes from 9N to 43N. Some of the earlier observations were made from a U. S. Navy PBY-6A (Catalina) aircraft while the remainder were made from a Navy R4D (DC-3, or Dakota).

2. Methods of observation and reduction of data

The methods of obtaining and reducing the data to values of heat flux have been described in *Exploring*

[1] Contribution No. 1031 from the Woods Hole Oceanographic Institution. This research was conducted under a contract with Office of Naval Research.

the Atmosphere's First Mile, edited by Lettau and Davidson, 1957. In this work, the vertical-velocity equation is derived as

$$w_i = a\Delta n/\rho V - b\Delta V/\rho V^2 - V\Delta\alpha_{att} + \sum_0^{t_i} \Delta n \Delta t + w_0. \quad (1)$$

The equation gives the vertical velocity w_i at the instant t_i in terms of the following: Δn, the vertical acceleration; ΔV, the deviations of the airspeed from the mean; $\Delta\alpha_{att}$, the deviation of the altitude of the airplane from the mean; and w_0, the airplane vertical velocity at the beginning of the run. One fifth-second averages of the observations were used in (1) to obtain a time series of w_i. Most of the runs lasted 2 min, although some of the earliest runs lasted only 30 sec.

The turbulent flow of sensible heat through a horizontal surface at the height, z_0, may be defined as

$$H \equiv c_p\overline{\rho w' T'} \quad (2)$$

when $\overline{\rho w'} = 0$. Here, w' is the vertical component of a gust velocity, and T' is the temperature deviation from the mean at z_0. In the present study, series have been obtained of observed values of w_i, the vertical velocities of the gusts measured according to equation (1), and T_i, the air temperatures, measured with a thermopile mounted on the airplane. The values in a given series were not obtained at a constant height, z_0, but at varying heights, $z_0 + \Delta z_i$, depending upon the altitude of the airplane. Under these conditions, the heat flux is redefined by the following form of the heat-flux expression:

$$c_p\overline{\rho w' T'} = c_p\overline{[\rho_i + f_\rho(\Delta z_i)][w_i - at - \bar{w}_i - f_w(\Delta z_i)] \times [T_i - bt - \bar{T}_i - f_T(\Delta z_i)]}. \quad (3)$$

Here, $f_\rho(\Delta z_i)$, $f_w(\Delta z_i)$, and $f_T(\Delta z_i)$ represent corrections to the observed values of ρ_i, w_i, and T_i obtained at $z_0 + \Delta z_i$ to make the values applicable to the reference height, z_0. The terms at and bt are the products of the slopes of the lines of regression of w_i and T_i against time. These terms are required since any short series of observations made in the atmosphere always will have a trend due to fluctuations with a period longer than the duration of the observations.

Equation (3) could be used for the computations of the heat flux in the atmosphere, but it will be shown now that a much simplified expression can be found that introduces errors of less than 2 per cent. First, it is necessary to show that the altitude of the airplane varies only a small amount during a two-minute observing flight. Root-mean-square altitude deviations were computed for several flights as a measure of the variation. The most extreme altitude variation observed during the entire program yielded an rms value of 16 m. Other values obtained in very rough, unstable air off the east coast were less than one-half of this value—*i.e.*, around 4 to 8 m. In the more stable air of the trade winds, the rms height values dropped to 1 or 2 m.

Using these figures, the results of neglecting the correction terms can be investigated. Considering first $f_\rho(\Delta z_i)$ a displacement, Δz_i, of 10 m in an atmosphere with an adiabatic lapse rate gives a temperature change of 0.1C and a value for $f_\rho(\Delta z_i)$ of 0.0004 kg m^{-3}. As this value is less than $\frac{1}{10}$ of a per cent of the density of the air in the regions studied, it can be neglected safely.

A single vertical-velocity measurement, w_i, is an average over the area of 360 m^2 which is the area swept out by an airplane wing in $\frac{1}{5}$ second. This area defines the horizontal dimensions of the gusts measured, and it may be assumed that the gust has comparable vertical dimensions. For the small vertical displacements that the airplane undergoes during its flight, the value of the gust at the reference level z_0 is included in the measured average. From the values of rms vertical velocities entered in table 1, it is seen that the vertical velocities vary slightly with height; hence, the value of $f_w(\Delta z_i)$ will be very small. Although the magnitude of $f_w(\Delta z_i)$ is very small, it cannot be dropped without first investigating the correlations that arise between it, T_i, and $f_T(\Delta z_i)$.

To evaluate the magnitude of the error in a heat flux determination resulting from correlations between the velocity and temperature, corrections and the gust velocities, densities, and temperature deviations, the following computation has been made. A gust has been assumed varying sinusoidally with a velocity amplitude of 100 cm sec^{-1} and a temperature amplitude of 0.3C in phase with the velocity and with a period of 4 sec. An atmosphere with an adiabatic temperature lapse rate and with an increase of rms vertical velocity of 20 cm sec^{-1} per 100 m is assumed. The height variation of the airplane was computed from the known characteristic response of the airplane, assuming no change in attitude and no horizontal component of the gust. It is found that the altitude reaches a maximum at 2.7 sec with an amplitude of 76 cm. The values of w_i, T_i, and ρ_i that would be observed from the airplane flying this path through the assumed gust were computed. The heat flux was computed by using this series of values and compared with the heat flux, $c_p\overline{\rho w' T'}$ being computed from the originally assumed values. The difference between the two computations was found to be less than one per cent. The flux was recomputed by using the average value of the density rather than the instantaneous observed value, ρ_i. The heat flux computed in this manner differed from the original flux, $c_p\rho\overline{w'T'}$, by only 1.2 per cent. From these computations, it is concluded that an error of only one or two per cent is introduced by neglecting corrective terms and using

TABLE 1. Airplane observations of temperature, humidity, turbulence, and fluxes.

Case I

17 December 1953, 1600 to 1620 EST, Region 1, 42.5N–68.5W, winds 325°, 7.8 m sec^{-1}, overcast, snow showers.

Height m	Pot. temp. K	Mix. ratio g kg^{-1}	σ_w cm sec^{-1}	σ_T C	$c_p\rho\overline{w'T'}$ mcal cm^{-2} sec^{-1}	$\rho\overline{w'q'}$ μg cm^{-2} sec^{-1}	$L\rho\overline{w'q'}$ mcal cm^{-2} sec^{-1}
0	283	8	—	—	—	—	—
140	267.7	1.2	93	0.39	6.0	—	—
280	267.1	1.2	96	0.21	4.5	0.5	0.3
560	267.0	1.2	131	0.33	6.0	2.0	1.2

Case II

23 December 1953, 1300 to 1325 EST, 42.5N–68.5W, Region 1, winds 284° 13.9 m sec^{-1}, 7/10 sky coverage by cumulus clouds.

0	282	7	—	—	—	—	—
50	277.4	—	54	0.21	0.3	—	—
150	277.6	—	68	0.15	0.9	—	—
290	278.1	—	82	0.18	1.5	—	—
580	277.3	—	87	0.18	0.3	—	—
840	278.1	—	39	0.30	−1.2	—	—
1620	287.5	—	12	0.09	0.0	—	—

Case III

5 January 1954, 1205 to 1230 EST, Region 1, over water north of Provincetown, Mass., winds 267° 6.3 m sec^{-1}, cirrus overcast.

0	278	5	—	—	—	—	—
15	272.5	2.9	44	0.27	2.1	—	—
45	272.5	2.9	50	0.21	1.5	—	—
95	272.8	3.1	39	0.15	0.6	—	—
150	272.9	3.0	53	0.18	1.2	0.1	0.07
305	272.9	3.1	33	0.24	−0.9	0.4	0.3
440	274.0	2.2	15	0.12	0.0	0.1	0.04
610	280.8	2.9	16	0.30	0.0	—	—
915	284.5	3.0	12	0.33	0.3	—	—

Case IV

7 January 1954, 1300 to 1320 EST, Region 1, 42.5N–68.5W, winds 309° 6.5 m sec^{-1}, cumulus overcast.

0	281	7	—	—	—	—	—
55	275.5	—	69	0.15	1.5	—	—
140	275.5	—	79	0.30	4.8	—	—
270	275.5	—	58	0.15	0.6	—	—
550	275.7	—	98	0.18	3.0	—	—
740	276.0	—	46	0.15	−1.2	—	—

Case V

29 January 1954, 1445 to 1530 EST, Region 1, 42.5N–68.5W, winds 307° 6.9 sec^{-1}, 2/10 sky coverage by cumulus.

0	278	5	—	—	—	—	—
85	265.8	1.5	92	0.42	5.7	—	—
185	266.0	1.5	108	0.63	10.5	0.1	0.1
340	266.4	1.4	121	0.24	6.6	0.7	0.4
630	266.3	1.4	44	0.39	2.7	−0.4	−0.2
875	269.8	0.2	18	0.30	−0.9	—	—
1140	271.5	0.2	16	0.15	0.3	—	—

TABLE 1—*Continued.*

Case VI

24 February 1954, 1420 to 1520 EST, Region 2, Weather Ship 'H' 36N–70W, winds 285° 8.2 m sec^{-1}, 8/10 sky coverage by cumulus clouds.

Height m	Pot. temp. K	Mix. ratio g kg^{-1}	σ_w cm sec^{-1}	σ_T C	$c_p\rho\overline{w'T'}$ mcal cm^{-2} sec^{-1}	$\rho\overline{w'q'}$ μg cm^{-2} sec^{-1}	$L\rho\overline{w'q'}$ mcal cm^{-2} sec^{-1}
0	289	12	—	—	—	—	—
30	288.3	5.2	52	0.30	2.7	—	—
60	288.1	5.0	64	0.27	2.4	—	—
180	288.5	4.8	57	0.12	1.2	—	—
330	288.3	4.8	57	0.09	0.3	—	—
610	288.2	4.5	93	0.27	0.3	—	—
915	289.4	4.8	40	0.24	−0.3	—	—
1220	289.5	3.8	35	0.45	0.6	—	—
1585	293.3	2.2	22	0.33	−1.8	—	—
2135	298.7	2.0	14	0.54	1.2	—	—

Case VII

14 January 1955, 1455 to 1535 EST, Region 1, 41.1N–71.5W 20mi. SE of Block Island, winds 340° 20.5 m sec^{-1}, clear.

0	279	6	—	—	—	—	—
60	273.3	1.2	74	0.55	2.6	—	—
150	273.0	1.2	133	0.12	0.2	10.8	6.5
305	272.5	1.0	96	0.12	−0.3	1.5	0.9
610	273.0	0.9	45	0.08	−0.3	0.0	0.0
915	273.5	0.9	89	0.26	−0.3	—	—
1220	275.0	1.0	19	0.11	−0.4	—	—
1220	279.0	1.0	44	0.30	−0.9	—	—

Case VIII

18 January 1955, Regions 1 and 2, Rhode Island to Bermuda, winds 307° 11.7 m sec^{-1}.

Series 1: 100 km offshore, 1305 to 1320 EST, 4/10 sky cover by cumulus clouds.

0	276	6	—	—	—	—	—
150	270.2	1.9	94	0.08	1.1	—	—
335	270.4	1.7	121	0.07	1.7	—	—
520	270.5	1.6	86	0.05	0.1	—	—

Series 2: 270 km offshore, 1350 to 1400 EST, complete stratocumulus overcast.

0	283	8	—	—	—	—	—
150	274.1	—	135	0.19	3.9	—	—
305	274.5	—	107	0.08	1.1	—	—

Series 3: 530 km offshore, 1455 to 1505 EST, 10/10 overcast.

0	290	12	—	—	—	—	—
120	282.5	5.9	177	0.18	1.3	—	—
460	282.0	6.0	174	0.10	2.1	—	—

Series 4: 800 km offshore, 1550 to 1610 EST, breaks in overcast.

0	289	11	—	—	—	—	—
120	286.7	6.6	138	0.11	2.1	—	—
305	286.2	6.0	134	0.10	2.0	15.0	9.0
550	286.2	5.5	122	0.09	1.1	15.0	9.0

Series 5: 1000 km offshore, 100 km NW Bermuda, 1650 to 1710 EST, 6/10 cumulus.

0	289	12	—	—	—	—	—
90	288.0	6.0	138	0.13	2.4	—	—
305	288.4	4.9	151	0.08	1.1	19.0	11.5
550	288.5	5.6	129	0.07	0.8	6.6	4.0

TABLE 1—*Continued.*

Case IX

20 January 1955, 1030 to 1055 AST, Region 2, 32.5N–65.0W NW of Bermuda, winds 320° 22.0 m sec^{-1}, 8/10 sky coverage by cumulus and cumulonimbus.

Height m	Pot. temp. K	Mix. ratio g kg^{-1}	σ_w cm sec^{-1}	σ_T C	$c_p\rho\,\overline{w'T'}$ mcal cm^{-2} sec^{-1}	$\rho\,\overline{w'q'}$ μg cm^{-2} sec^{-1}	$L\rho\,\overline{w'q'}$ mcal cm^{-2} sec^{-1}
0	292	13	—	—	—	—	—
60	290.3	—	98	0.15	1.1	—	—
150	289.8	—	87	0.08	0.6	—	—
305	290.8	—	111	0.10	1.3	—	—
610	291.4	—	65	0.09	0.6	—	—

Case X

22 January 1955, 1310 EST, Region 1, 39N–69W, wind 270° 6.0 m sec^{-1}, 8/10 sky coverage by post cold-frontal cumulus clouds.

0	286	10	—	—	—	—	—
100	278.8	—	61	0.11	−0.4	—	—
300	280.0	—	—	—	—	—	—

Case XI

7 December 1955, Bermuda to Rhode Island, winds 360° 1 m sec^{-1}, 4/10 sky coverage by cumulus clouds.
Series 1: 1200 to 1220 EST, Region 2, 600 km offshore.

0	292	13	—	—	—	—	—
15	284.6	—	67	0.18	2.1	—	—
60	284.4	—	98	0.15	2.8	—	—
140	284.7	—	96	0.10	1.8	—	—
325	284.8	—	102	0.10	1.5	—	—
565	284.7	—	92	0.08	0.5	—	—

Series 2: 1310 to 1330 EST, Region 1, 300 km offshore.

0	290	13	—	—	—	—	—
15	278.1	—	54	0.14	1.1	—	—
60	278.2	—	71	0.10	1.0	—	—
150	278.3	—	89	0.08	1.1	—	—
300	277.6	—	78	0.06	0.4	—	—
600		—	55	0.09	−0.1	—	—

Series 3: 1430 to 1450 EST, Region 1, 100 km offshore.

0	283	8	—	—	—	—	—
60	273.0	—	78	0.10	1.2	—	—
150	272.9	—	77	0.08	0.5	—	—
300	272.8	—	72	0.06	0.4	—	—
600	273.4	—	58	0.05	0.2	—	—

Case XII

9 March 1956, 1215 to 1310 EST, Region 1, 39.5N–70.5W, winds 275° 6.8 m sec^{-1}, 6/10 sky coverage by cumulus clouds.

0	280	7	—	—	—	—	—
60	275.0	2.8	86	0.17	1.9	(5.6)	(3.4)
200	275.1	2.7	105	0.14	0.5	—	—
305	275.3	2.7	92	0.10	1.0	—	—
610	274.9	2.7	85	0.07	0.8	—	—
940	277.6	1.7	45	0.30	−0.7	—	—

TABLE 1—*Continued.*

Case XIII

11 August 1956, Region 3, 19N–66W, 550 km ahead of hurricane Betsy.

Series 1: 1135 to 1225 AST, wind 058° 8.7 m sec^{-1}, 3/10 sky coverage by cumulus.

Height m	Pot. temp. K	Mix. ratio g kg^{-1}	σ_w cm sec^{-1}	σ_T C	$c_p\rho\,\overline{w'T'}$ mcal cm^{-2} sec^{-1}	$\rho\,\overline{w'q'}$ μg cm^{-2} sec^{-1}	$L\rho\,\overline{w'q'}$ mcal cm^{-2} sec^{-1}
0	300	24	—	—	—	—	—
8	299.0	18.4	26	0.12	0.5	—	—
15	299.0	18.3	29	0.10	0.2	—	—
30	299.1	18.0	53	0.10	0.3	—	—
60	299.1	18.1	43	0.08	−0.1	—	—
150	299.5	17.9	40	0.07	0.2	1.5	0.9
305	299.4	17.5	48	0.12	0.4	5.1	3.2
610	299.8	16.3	33	0.20	0.2	5.6	3.3
1005	301.1	13.3	36	0.21	−0.5	2.3	1.2

Series 2: 1335 to 1410 AST, wind 060° 9.0 sec^{-1}, 3/10 sky cover by cumulus.

0	300	24	—	—	—	—	—
15	299.4	18.1	29	0.07	0.2	—	—
30	299.4	18.1	37	0.06	0.2	—	—
60	299.5	18.3	48	0.08	−0.3	—	—
150	299.6	18.0	50	0.05	0.2	5.8	3.4
305	299.6	17.4	52	0.14	0.4	3.2	1.9
610	299.9	16.2	37	0.34	−0.1	5.6	3.3

Case XIV

15 August 1956, 1030 to 1130 AST, Region 2, 19N–66W, wind 080° 8.5 m sec^{-1}, 3/10 sky coverage by small cumulus clouds.

0	300	24	—	—	—	—	—
15	299.7	20.4	27	0.11	0.3	—	—
30	299.6	19.9	28	0.08	0.1	—	—
60	299.7	19.9	40	0.08	0.1	—	—
150	300.0	19.5	33	0.07	0.0	1.0	0.6
305	299.6	18.9	39	0.08	−0.1	1.6	0.9
490	299.9	18.3	25	0.21	−0.3	1.8	1.0

Case XV

16 August 1956, 0735 to 0830 AST, Region 3, 19N–66W, wind 035° 5.2 m sec^{-1}, showery, 6/10 sky coverage cumulus and cumulonimbus.

0	300	24	—	—	—	—	—
30	299.0	18.9	30	0.07	0.2	—	—
60	299.1	18.9	44	0.06	0.1	—	—
150	299.8	18.6	44	0.04	0.2	0.7	0.4
305	299.8	17.8	26	0.05	0.0	0.9	0.5
470	299.7	17.6	20	0.08	−0.1	−0.1	−0.1

Case XVI

20 August 1956, 1725 to 1810 AST, Region 4, 13N–59W, wind 080° 4.8 m sec^{-1}, 4/10 sky coverage by cumulus clouds.

0	300	24	—	—	—	—	—
15	299.9	18.8	29	0.05	0.1	—	—
30	299.9	18.0	29	0.04	0.0	—	—
60	300.0	18.0	28	0.03	0.0	—	—
150	299.9	18.0	44	0.05	−0.1	—	—
305	299.7	17.3	50	0.04	−0.1	1.7	1.0
610	300.3	16.2	26	0.15	0.0	3.1	1.8

TABLE 1—*Continued.*

Case XVII

21 August 1956, 1445 to 1520 AST, Region 4, 12N–57W, wind 080° 6.8 m sec^{-1}, 7/10 sky coverage by cumulus and cumulonimbus in weak disturbance in easterlies.

Height m	Pot. temp. K	Mix. ratio g kg^{-1}	σ_w cm sec^{-1}	σ_T C	$c_p\rho\,\overline{w'T'}$ mcal cm^{-2} sec^{-1}	$\rho\,\overline{w'q'}$ μg cm^{-2} sec^{-1}	$L\rho\,\overline{w'q'}$ mcal cm^{-2} sec^{-1}
0	300	24	—	—	—	—	—
15	298.9	18.8	29	0.08	0.0	—	—
30	299.0	18.4	29	0.05	0.1	—	—
60	298.9	18.4	41	0.06	0.2	—	—
150	299.4	17.8	42	0.08	−0.2	−3.8	−2.3
305	299.4	17.7	31	0.05	−0.2	—	—
455	299.8	17.2	20	0.06	−0.1	2.5	1.5

Case XVIII

24 August 1956, 1110 to 1155 AST, Region 4, 11.5N–59.5W, wind 0.80° 7.2 m sec^{-1}, 4/10 sky coverage by cumulus clouds.

0	300	24	—	—	—	—	—
15	300.1	18.0	26	0.05	0.1	—	—
30	300.1	18.0	32	0.05	0.1	—	—
60	300.1	18.0	39	0.06	0.0	—	—
150	300.3	17.4	45	0.05	−0.4	1.5	0.9
305	300.2	16.6	45	0.10	−0.1	4.3	2.5
575	300.1	16.0	42	0.20	−0.2	5.7	3.3

Case XIX

15 November 1957, 1248 to 1258 AST, Region 4, 9N–58W, wind 080° 8.0 m sec^{-1}, 4/10 sky coverage by cumulus clouds.

0	301	25	—	—	—	—	—
60	299.8	18.7	33	0.22	0.4	—	—
150	300.2	18.6	28	0.10	−0.3	0.9	0.5

Case XX

22 February 1958, 1440 to 1455 AST, Region 3, 19N–64W, wind 040° 9.8 m sec^{-1}, 5/10 sky coverage by cumulus clouds.

0	297	20	—	—	—	—	—
30	295.7	13.5	70	0.06	0.4	—	—
150	296.0	13.0	97	0.08	−1.9	12.1	7.3
300	295.8	12.7	73	0.05	−0.2	−8.2	−4.9

Case XXI

24 February 1958, 1102 to 1150 AST, Region 4, 11N–60W, wind 050° 5.0 m sec^{-1}, 8/10 sky coverage by cumulonimbus and cumulus clouds.

0	299	22	—	—	—	—	—
30	297.8	17.0	38	0.06	0.1	—	—
125	298.0	15.9	56	0.09	−0.6	0.7	0.4
320	298.3	16.3	41	0.09	−0.2	0.3	0.2
555	298.3	15.7	52	0.09	−0.7	3.0	1.8
800	299.2	13.5	59	0.08	0.1	1.4	0.8
1120	301.9	11.2	46	0.06	−0.1	−1.8	−1.1

Case XXII

25 February 1958, 0946 to 1115 AST, Region 4, 11N–60W, wind 070° 8.0 m sec^{-1}, 5/10 sky coverage by cumulus clouds.

0	299	22	—	—	—	—	—
30	297.9	16.9	68	0.07	−0.6	—	—
165	298.0	16.7	50	0.06	−0.1	1.7	1.0
470	298.4	15.5	55	0.13	−1.4	4.4	2.6
900[1]	299.8	12.4	37	0.22	−0.1	0.5	0.3
900	299.8	14.9	50	0.09	−1.0	4.2	2.5
960[2]	300.2	13.6	136	—	—	25.0	15.0
1200[3]	300.5	11.3	71	0.13	−2.2	−4.8	−2.9

[1] Flight under an overhanging section of cumulus cloud.
[2] Flight through a cumulus cloud.
[3] Flight between the tops of two small cumulus clouds.

the average value of the density of air. Hence, the sensible heat flux may be expressed by the following equation:

$$c_p\overline{\rho w'T'} \approx c_p\bar{\rho}\overline{(w_i - at - \bar{w}_i)(T_i - bt - \bar{T}_i)}. \quad (4)$$

A form better suited for computation is obtained by multiplying, averaging, and simplifying with the identity $\overline{atT_i} = \overline{btw_i} = ab\bar{t^2}$. We get the following equation which has been used in all computations:

$$c_p\overline{\rho w'T'} \approx c_p\bar{\rho}(\overline{w_iT_i} - \bar{w}_i\bar{T}_i - ab\bar{t^2}). \quad (5)$$

Similar equations are used for computation of σ_w, σ_T, and $\overline{\rho w'q'}$.

The probable error of flux determinations cannot be established for all conditions, since the error depends on the range of sizes of the gusts producing the transport. If the gust sizes are all within the size range of 20 m to 6 km, the airplane and the instruments would respond completely and the necessary data would be recorded with good accuracy. The errors present would be small and caused by airplane deformation, reading, and calibrating errors. Probable errors under these circumstances would be about 5 per cent for the heat flux. Whenever a significant portion of the total transport is carried by gusts smaller than 20 m or larger than 6 km, the determined values will be too small. From studies made by Panofsky and McCormick (1954) of the spectra of turbulence at 100 m at the Brookhaven tower, it is concluded that very little transport is accomplished by gusts smaller than 20 m. Gusts larger than 6 km may transport significant amounts of heat and water vapor, but little is known about transport in this spectral region. As a check upon transport by large gusts and the over-all accuracy of the airplane measurements, the average of a series of heat-flux determinations made over Long Island was compared with the total heat accumulated in the air mass as it moved across the island. The agreement was within 4 per cent, indicating good accuracy of the method and that transport by gusts outside the 20 m-to-6 km range was small in this case. It cannot be said, however, that transport by gusts outside the specified size range will be small in all cases.

Comparisons of the heat fluxes measured from the airplane with fluxes measured from ground-based instruments at O'Neill, Nebraska (Lettau and Davidson, 1957) showed that the airborne instruments gave values 60 per cent too small. Heat fluxes measured over the Gulf of Maine also were only one-third of the fluxes computed from observations of the initial and final temperature soundings along air trajectories. It was concluded that the mass of the thermopile housing increased the effective lag of the thermopile and seriously decreased the measured amplitude of the temperature variations. Consequently, a correction factor of three has been applied to the data of the first six cases. No other corrections have been applied to any data in this paper. A new thermopile and housing were constructed which were less massive, better-ventilated, and utilized smaller thermocouple wire. This thermopile has a response time of about 0.2 sec at aircraft speeds.

Mixing-ratio values used in the computation of water-vapor flows were determined from wet- and dry-bulb thermistors exposed to the free air stream in a venturi housing. The thermistors, No. 31D4 of Victory Engineering Corporation, have a thermal response time of about one second when mounted in the housing and ventilated at airplane speeds. Since this response time is greater than the response time of the velocity-measurement system, individual mixing-ratio values were matched for multiplication with the average velocity for the preceeding five fifth-second intervals. Values were read from the record every second giving 120 values per run. For sub-freezing temperatures, a lithium-chloride strip was used to measure humidities and similarly matched with velocities averaged over one second.

The contribution of the high-frequency end of the transport spectrum is lost by the slow response of the thermal elements. Comparisons were made between the fluctuations in mixing ratio as measured by the thermistors and as measured by a University-of-Texas-model refractometer. The refractometer measurements, made under the direction of R. M. Cunningham of Geophysical Research Directorate while a C-130 was flying off the wing tip of the R4D in the trade-wind region, confirmed the suspicion that the fluctuations of mixing ratio were too fast to be recorded reliably by the thermistors at the 30-m level. At the 150-m level, the fluctuations have a predominant wave length in the 100- to 500-m range. The thermistors can respond satisfactorily to fluctuations of this scale when flown through these regions at 60 m sec^{-1}. Hence, only those water-vapor flux measurements made above the 150-m level have been included in this report.

3. Presentation of data

The reduced data for the 22 cases studied have been collected in table 1. For each case, the date, time, location, wind, and cloudiness are given in the heading. The winds were observed from drift-sight readings or rawin reports and represent averages through the layer studied. Potential temperatures and mixing ratios at zero height are values for the air in immediate contact with the water as determined from ship reports of the water temperature.

4. Turbulent vertical velocities

The root-mean-square vertical velocities, σ_w, are presented in table 1 as a measure of the air mass's degree of turbulence and kinematic ability to transport properties vertically. Inspection of the values listed shows considerable variation from day to day and region to region. A variation which is noted in nearly every case is an increase in intensity upward through the lowest levels, a broad maximum in the lower half of the ground layer, and a decrease in the upper half of the ground layer and the inversion or cloud layer. In cases of greater instability, the maximum velocities are displaced higher toward the top of the ground layer. When the horizontal turbulent velocities, which were measured but not listed in table 1, are combined with the vertical velocities to form an rms total turbulent velocity vector, the height variation transforms into a distribution with a maximum at the lowest levels and a gradual diminution of intensity up into the cloud layer.

These distributions are interpreted to be the result of both the production of turbulence near a surface and the damping of the vertical component of the gust near a surface and in the stable air aloft. The upward displacement of the maximum vertical velocities in the unstable case results from the buoyancy acceleration of warm air parcels. Another source of turbulence is the buoyancy associated with the condensation of water vapor in cumulus clouds. This type of motion originates near the condensation level of the air mass. The vertical velocities first increase to a maximum of several m sec^{-1} and then decrease rapidly whenever a stable layer is penetrated. If all three sources of turbulence are equally effective in a given air mass, the resulting distribution of turbulence will be very complex. However, many cases in table 1 represent a predominance of one or two sources of turbulent energy. Case XI is an excellent example of pure convective turbulence, since the water was warmer than the air and the wind was only about 1 m sec^{-1}. Many observations taken in Region 1 represent a combination of mechanical and convective turbulence. In the trade-wind region where the air-sea temperature difference is slight, only mechanical and condensation-convective turbulence is important in producing the observed vertical-velocity profile. Here the moderate values of the turbulence observed in the sub-cloud layer are the consequence of the absence of convection, the moderate winds, and the inability of the turbulence of the cumulus clouds to penetrate the air beneath them.

No theory has been developed to treat the interrelation of the different types of turbulence, but the uncomplicated situation of heating from below in the

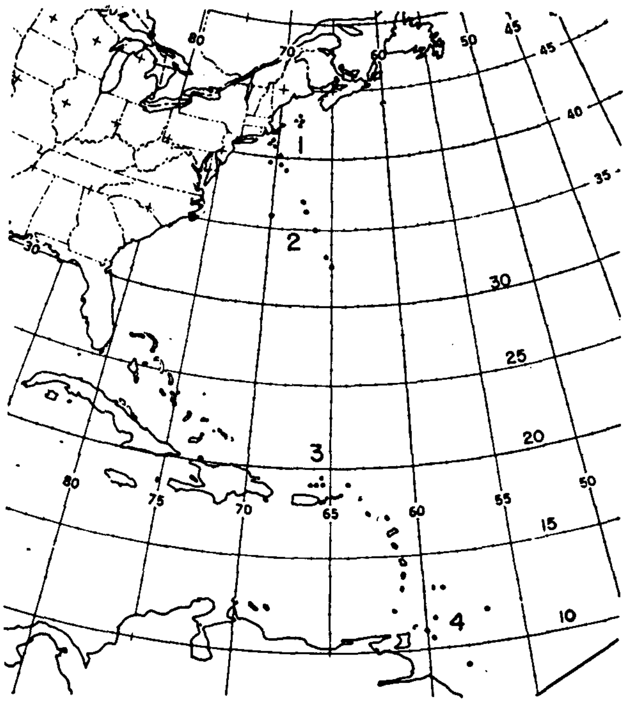

FIG. 1. Map of western North Atlantic Ocean. Dots represent location of observations. Figures identify regions mentioned in text.

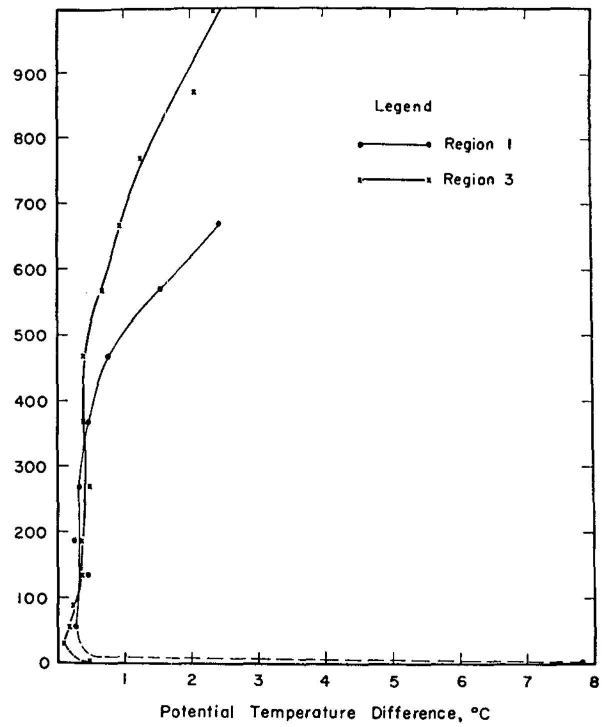

FIG. 2. Potential-temperature difference-height diagram. Average temperature differences of table 2 for Regions 1 and 3 are plotted to show potential-temperature minimum.

absence of a mean wind has been studied by Malkus (1954). His theory determines the heat transport through a fluid contained between a heated horizontal surface and an upper cooled parallel surface. The transport is given in terms of the smallest eddy size representing the stability restrictions on the fluid motion.

The mean total turbulent velocities may be predicted from the theory and compared with the observations of case XI. Malkus' equation gives $\overline{V \cdot V} = \frac{1}{9}(K/h)^2\lambda$ where $\lambda \equiv \alpha g \beta_0 h^4/K\nu$. Here, h is the height of the layer of unstable air considered; K is the thermometric conductivity of air; α is the coefficient of thermal expansion of air; β_0 is the mean negative temperature gradient between the sea surface and the height, h; ν is the kinematic viscosity of air; and g is the acceleration of gravity. The space average of the squared turbulent velocities $\overline{V \cdot V}$ is thus a function of the gradient, the dimensions of the layer, and the molecular properties of air. In case XI, the air-sea temperature difference was about 10C, the wind only about 1 m sec^{-1}, the height of the unstable air about 300 m, and the total rms turbulent velocities were found to reach a maximum of 180 cm sec^{-1}. When the dimensions of the system and the temperature difference are entered in the equation, an upper limit to rms total velocity of 520 cm sec^{-1} is found. The agreement between the two values is fair enough to encourage further exploration of the theory. The small observed velocities may be explained by the stable air aloft which is capable of damping the turbulent gusts which enter from below, while the theory was developed on the basis of a solid lid at the upper boundary.

5. Sensible heat flux

Convergence of heat flux. An upward flux of sensible heat was observed in all but two cases in the lowest layers of unstable air above the warmer water. In these two cases (X and XXII), observations were not made low enough to be in the unstable layer, and, hence, downward fluxes were observed. In sixteen cases, the direction of the heat flux reversed with height so that at the upper stable levels the flux was directed downward. In the remaining four cases, the soundings were terminated at 550 m to 610 m for operational reasons. A convergence of sensible heat into the ground layer is produced by the decrease to zero of the upward flux and the increase in downward flux with height. Thus, the air in this layer is heated both by the heat transported upward from the water and by the heat transported downward from the warm air of the subsidence inversion. In the middle latitudes, a greater proportion of the heat expended in warming the air is derived from the ocean. In the lower latitudes, a greater proportion of sensible heat is derived from the warm air aloft.

Persistence of potential temperature minimum. A cold subsiding continental air mass has a stable lapse rate before it begins moving southward over the warm land or the ocean. Over the ocean, the lowest layer is heated rapidly, thus producing a potential-temperature curve with a minimum at some relatively low level. If the convergence of heat into the air mass is equal at all levels, then the temperature profile will retain the minimum at a low level as the air mass travels southward. To determine whether this occurs in the air masses under study, averages of the potential temperatures in several height ranges were found for four different geographical regions. The four regions, shown in fig. 1 (*i.e.*, (1) offshore New England, (2) Bermuda, (3) Puerto Rico trade-wind region, and (4) Trinidad trade-wind region), represent different downstream positions or durations over the ocean. In table 2, the average differences in potential temperature from the minimum temperature of an individual sounding are tabulated. No averages are given whenever one or more of the cases used had no values available in a given height range. Sea temperatures are given since they represent the temperature of the air in contact with the water. The shape of the temperature profile from the ocean surface to the lowest level given in the table is not known, but it can be inferred from other studies in micrometeorology to be strongly super-adiabatic in the lowest meter and less unstable at higher levels. Fig. 2 has been drafted to show this feature graphically. The table shows that the air in the level from 20 m to roughly 300 m has a lower potential temperature than the air in contact with the water below or the air above it in all four regions, indicating that the diffusion processes in combination with radiative processes operate in such a manner as to produce equal convergence in each layer.

Table 2. Average potential-temperature differences.

Height range in meters	Region 1	Region 2	Region 3	Region 4
0 (sea temp)	7.8	3.30	0.48	1.30
20 to 40	—	—	0.10	—
40 to 70	0.26	—	0.19	0.16
70 to 110	—	0.15	0.22	0.35
110 to 160	0.44	0.20	0.38	0.49
160 to 220	0.24	0.44	0.39	0.38
220 to 320	0.32	0.52	0.48	0.39
320 to 420	0.46	0.71	0.36	0.55
420 to 520	0.72	0.69	0.36	0.71
520 to 620	1.54	0.92	0.67	0.80
620 to 720	2.40	1.12	0.92	1.27
720 to 820	—	—	1.22	1.46
820 to 1020	—	—	2.04	2.44
1020 to 1220	—	—	2.38	3.48
1220 to 1620	—	—	4.80	5.05

Fluxes interpreted by theories of heat transport. The several physical processes operating in a moving air mass heated both from below and above interact strongly and cannot be described completely by any existing theory. No attempt will be made here to review the vast field of transport theory but rather to discuss a few works that help interpret the fluxes observed in the present study.

The theory of heat diffusion developed by Taylor (1915) and Schmidt (1921) states that heat will be transported by turbulence down a potential-temperature gradient with a magnitude proportional to the gradient and a diffusion parameter. Table 1 shows that the majority of the fluxes conform to this theory in so far as the direction is concerned. As the theory cannot specify the diffusion factor for a given air mass, no magnitudes can be computed.

In many layers, it is noted that the flux is upward although the diffusion theory states that the flux should be downward. These observations are in agreement with the convective-turbulence theory of Priestley and Swinbank (1947). This theory states that the heat-diffusion equation is incomplete without a term depending upon the buoyancy of the individual parcels of air. The effect of this term is to allow an upward transport of heat through a stable atmosphere. This buoyancy effect attains importance under certain conditions of heating, turbulence, and parcel size which allow the parcel to receive and maintain an excess temperature for a sufficiently long time. Priestley (1954) extended this notion by developing equations which gave the heat flux in terms of the observed temperature fluctuations. Bunker (1956) has shown that these equations give values that are in good agreement with observed fluxes, using the observations contained in the present case VIII.

The theory of thermal turbulence developed by Malkus (1954) has been found capable of predicting the heat flux in case XI with order-of-magnitude accuracy. This theory gives a heat flux of 0.4 mcal cm^{-2} sec^{-1} while the observed fluxes averaged 1.1 mcal cm^{-2} sec^{-1} and ranged from 0.4 to 2.8 mcal cm^{-2} sec^{-1}. The theory also predicts rms temperature deviations of 0.05C, while the observed fluctuations ranged from 0.05C to 0.18C.

Regional variations. Averages were found for the upward flux by averaging all of the values at or below 60 m. If no observation was made at 60 m, the 150-m observation was used provided the air was still unstable at 150 m. The average downward fluxes were formed similarly from all of the observations taken in the stable layer above the level at which the flux changes sign. Excluded from this average are the two cloud flights of case XXII. The averages are entered in table 3 together with latent-heat-flux averages.

The most significant regional variation is noticed in the upward flux of sensible heat. The decrease from 2.3 mcal cm^{-2} sec^{-1} in Region 1 to 0.1 mcal cm^{-2} sec^{-1} in Region 4 is associated with the decrease of air-sea temperature differences from Region 1 to 4. This decrease directly affects the transport by decreasing

TABLE 3. Regional averages of sensible- and latent-heat fluxes.

	mcal cm^{-2} sec^{-1}		
Region	Upward sensible-heat flux	Downward sensible-heat flux	Latent-heat flux
1	2.30	0.39	1.08
2	2.00	0.08	8.38
3	0.17	0.46	1.54
4	0.10	0.32	1.17

the temperature gradient and indirectly affects it by decreasing the convective turbulence. The variation of the downward flux of heat is rather slight and suggests a compensating relation between gradient and turbulence. The ratio of the upward to the downward flux of sensible heat shows that in the first two regions the air is being warmed primarily by the heat derived from the ocean. In the tropical regions, nearly three times as much heat is diffused downward from the inversion air as is diffused upward from the sea surface.

A comparison has been made between the regional averages of upward heat flux and the averages determined by others in either the same region or meteorologically comparable regions. The values to be compared are presented in table 4 in calories cm^{-2}

TABLE 4. Comparisons of average sensible-heat fluxes.

	cal cm^{-2} day^{-1}					
Author:	Bunker	Jacobs	Budyko	Manabe	Miyazahi	Riehl
Method:	$c_p\rho\overline{w'T'}$	Em. For.	Em. For.	Integral	Em. For.	Em. For.
Region						
1	199	120W	82	555	180	—
2	182	70 to 260W	87	555	180	—
3	15	0	27	—	—	8 to 16
4	9	−5	3	—	—	—

day^{-1}. The averages given by Jacobs (1943) were computed from a vast number of ship reports of surface winds, air temperatures, humidities, and sea temperatures by use of empirical formulae relating these quantities to heat and water-vapor flow. The winter-season averages are entered in table 4 for Regions 1 and 2 since all of the present measurements were made in the winter time. For Regions 3 and 4, Jacobs' (1951) annual averages are used for comparison. Annual values computed by Budyko (1956) are presented in the next column. These were computed from ship reports by use of empirical formulae. The next three columns present values obtained not in Regions 1, 2, or 3, but in regions that are meteorologically similar. The values under the headings Manabe (1957, 1958) and Miyazahi (1949) were determined over the Japan Sea, which is similar to Regions 1 and 2. The fluxes of Riehl *et al.* (1951) were found from empirical formulae over the sea between San Francisco and Hawaii, an area which is similar to Region 3. The measurements of Manabe were made during January and February, 1955. Fluxes of sensible heat were obtained by an integral method which used radiosonde observations around the Sea to determine the amount of heat taken up by the air. The flux determined by Miyazahi was computed from empirical formulae and represents a five-year wintertime average.

Comparing the averages of Region 1, it is seen that the turbulence method gives a higher value than do the empirical formulae. Much of the difference comes from the fact that the averages of Jacobs and Budyko include winds from all directions. A fair agreement occurs between the values of Region 1 and 2 and those obtained over the Japan Sea. The value obtained by the turbulence method falls between the high value obtained by Manabe using the integral method and the low value obtained by Miyazahi using the empirical-formulae method. The downward flux of heat should be added to the upward flux to obtain a value to be compared to the total sensible-heat flux found by Manabe. The total flux obtained, 232 cal cm^{-2} day^{-1}, is still smaller than 555 cal cm^{-2} day^{-1} but not too small to be explained as the result of differences due to local variations or errors intrinsic in the methods of determination.

In the trade-wind region, excellent agreement is reached between the turbulence-method values and the values of Riehl determined in a comparable region of the Pacific Ocean trade winds. Riehl's observations were obtained from weather ships stationed between San Francisco, California and Hawaii during July through October, 1945. These observations are more reliable than the observations taken by commercial ships elsewhere. The values of Jacobs and Budyko disagree, but their average agrees well with the values of Riehl and Bunker. In Region 4, the magnitudes of the flux are small, and Jacobs indicates a flux of heat into the ocean.

6. Latent-heat fluxes

Regional variations. The latent-heat fluxes observed in the ground layer have been averaged and included in table 3. No values observed in the cloud layer are included in the average, as these fluxes would be unrepresentative of the turbulent flux from the sea surface since the upward flux in the cloud layer is strongly organized by the cumulus clouds into preferred cloudy areas. The increase of latent-heat flux from Region 1 to Region 2 is the result of the increased gradient caused by the warming of the air and the consequent increase in the ability of the air to retain water vapor. In Region 1, the saturation mixing ratio of the air varies from 2 to 5 g kg^{-1}, while in Region 2 the saturation mixing ratio is 10 to 15 g kg^{-1}. As the turbulence is about the same in the two regions, the air's ability to hold water vapor accounts for the difference in gradient and flux. The flux is much lower in Regions 3 and 4. Here, the low value must be attributed to the decrease in the magnitude of the turbulence, since the gradient of the moisture is nearly the same as in Region 2. Inspection of table 1 shows that the rms vertical velocities in the trade winds are one half or a third of the intensity in Region 2. In spite of the decreased latent-heat flux in the trades, it is about one order of magnitude larger than the sensible-heat flux.

TABLE 5. Regional averages of the latent-heat flux.

	cal cm^{-2} day^{-1}				
Author: / Method:	Bunker / $c_p\rho\,\overline{w'T'}$	Jacobs / Em. For.	Budyko / Em. For.	Manabe / Integral	Riehl / Em. For.
Region					
1	94	120? W	230	340	—
2	720	480 to 600W	330	340	—
3	132	200	275	—	250
4	100	<200	165	—	—

Table 5 has been compiled to compare the fluxes with those observed by Jacobs, Budyko, Manabe, and Riehl. With the exception of the average for Region 2, the turbulence method gives lower values than the other methods.

Local variations. Inspection of the water-vapor fluxes fails to show any systematic variation with height in the ground layer, but it shows a large range of fluxes from -8 to 19 $\mu g\ cm^{-2}\ sec^{-1}$. The possibility of this wide range resulting from instrumental difficulties or failures was eliminated by checking records, calibrations, and data reductions. About ten per cent of the observations show a flux opposed to the mean gradient of the mixing ratio. In these cases, the net flux for the particular flight was found to be dominated by the presence of one or more very dry or moist updrafts or downdrafts of relatively long duration indicating a sampling that was too small. Had the runs been 12 or 18 km long instead of 6 km, the range would have been decreased and the negative fluxes possibly eliminated.

Large dominating gusts appear to be associated with active cumulus or cumulonimbus clouds. Case VIII yielded the largest fluxes, and many active cumuli were building up and dissipating in the area. The value of -4 $\mu g\ cm^{-2}\ sec^{-1}$ was observed in case XVII at 150 m in the presence of cumulonimbus associated with a disturbance in the easterlies. The negative flux of case XX was observed in a modifying polar air mass that had penetrated into the trade-wind area.

The effect of cumulus clouds upon the flux of sensible heat and water vapor in both the cloud air and air surrounding the clouds was studied on 25 February 1958, case XXII. In addition to the regular flux measurements, three special flights were made through and near clouds. The first was made under the overhanging of a cumulus tilted by the shear of the wind, the second was through a cumulus cloud, and the last was between the tops of two small clouds. The first run gave an upward water-vapor flux that was much smaller than the flux obtained at the same level but far from the cloud. The records of vertical velocities and water vapor show that as the airplane passed under the overhang it penetrated a dry air parcel for 30 sec (2 km) which was ascending. When this negative flux is averaged with a positive flux observed in the remainder of the run (4 km), a small positive flux results. The cloud penetration yielded a large water-vapor flux as was expected. The flight between the cloud tops gave a rather large negative flux. Here again, the flux was dominated by a single intense gust. Further investigation of the association with clouds will have to be made before these gusts are understood and their origin established.

Comparison of fluxes with evaporation determined by formula. The empirical evaporation formula,

$$E = k(e_s - e_a)W_a,$$

was developed and used by Jacobs (1942) and others to compute the evaporation E, in mm day^{-1}, from the saturation water-vapor pressure above the ocean surface e_s, in mb, from the water-vapor pressure at anemometer level, e_a, and the wind speed, W_a, in m sec^{-1}. The value of the evaporation factor, k, was computed from the balance of energy received and lost by an air mass and was found to lie between 0.07 and 0.19. Jacobs has adopted $k = 0.14$ and computed values of evaporation for the North Atlantic and Pacific Oceans. The value 0.086 was found by Wüst from the METEOR observations to apply to the NE trade-wind region. Sverdrup (1951) gives a complete discussion of these values and the problems of evaporation measurement.

A comparison of the results of the formula method with the airplane fluctuation method was carried out in August 1956 in the trade-wind region north of Puerto Rico. Surface meteorological and oceanographical observations were made from the R/V CRAWFORD on three days when water-vapor-flux measurements were made from a PBY-6A flying overhead. The airplane technique gave evaporations 25 per cent smaller than the formula method when 0.086 was used for the value of k.

7. Heat and water-vapor accumulation

The process of the heat and water-vapor accumulation in the air masses studied undergoes several distinct phases which now may be summarized. Before a polar continental air mass reaches the ocean, its lowest layers are well mixed by mechanical and dry-

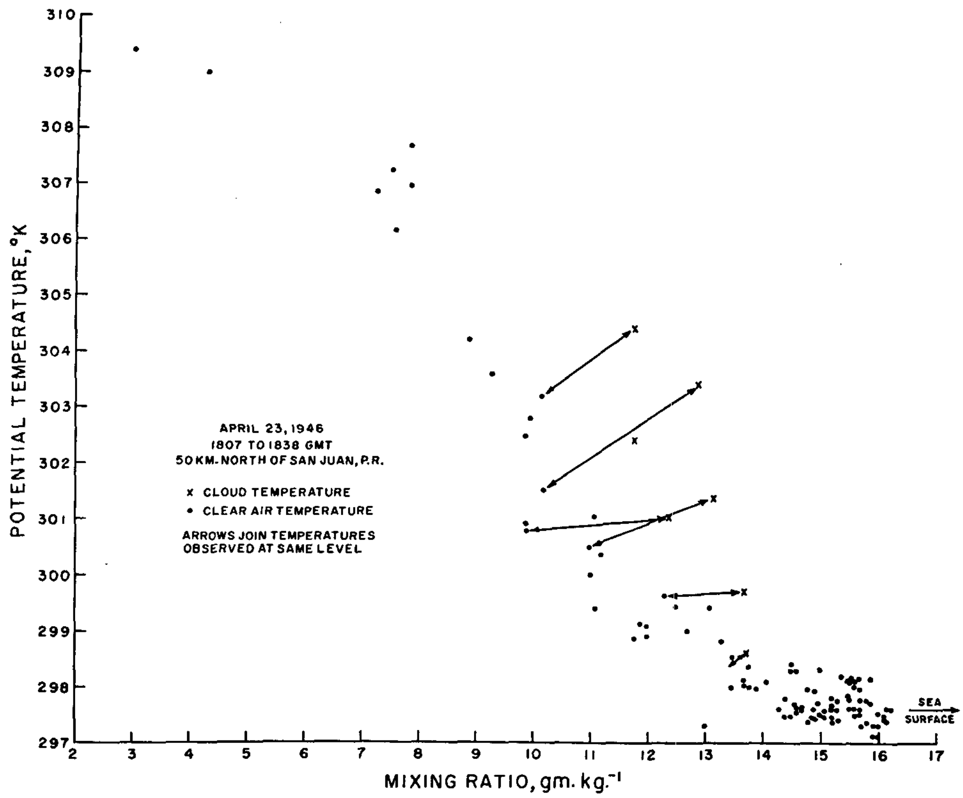

FIG. 3. Potential temperature-mixing ratio diagram of clear air and air within cumulonimbus cloud. The lines connect values inside and outside of the cloud at the same altitude.

convective turbulence. Heat is being transported upward in the mixed layer and downward in the smooth subsidence-inversion layer. Very small amounts of water vapor may be diffused upward from the ground. When the air mass moves out over the ocean, the sensible heat-flux pattern remains the same but an upward flow of water vapor is initiated or greatly accelerated. An approximate daily heat budget for winter-time polar air in this state at 45N may be made using average values of radiational loss and gain by London (1957). He finds a cooling of about 0.8C per day in the lowest kilometer. A flow of 2.1 mcal cm^{-2} sec^{-1} upward and 0.4 mcal cm^{-2} sec^{-1} downward into the layer gives a warming of 8.8C per day. Therefore, a net warming of 8.0C per day results from the summation of solar radiation, long-wave radiation exchange, and the turbulent transport of sensible heat. Neglected in this estimate is any warming due to air subsiding into the layer, any heating due to the condensation of water vapor, or loss of heat by transport to higher levels.

Dry-convective and mechanical turbulence continues as the diffusing agent until the turbulent ground layer air approaches saturation. At this stage, the buoyancy produced by the condensation of water vapor becomes an important factor in the acceleration of diffusion of heat and water vapor into the smooth air of the inversion layer. The change from mechanical and dry-convective turbulence to mechanical, dry- and moist-convective turbulence produces a change in the distribution of intensity of turbulence in the ground layer as well as in the inversion layer. In the ground layer, the turbulence increases moderately and the level of maximum intensity may rise. In the inversion air, the turbulence is increased one or two orders of magnitude locally where the cumulus clouds build up and a general moderate increase of turbulence occurs in the inter-cloud space. By this more rapid process, the atmosphere is heated and moistened to heights of many kilometers. The continuation of the cumulus activity creates a new cloud layer above the ground layer in the subsidence-inversion air. This layer is more moist and less stable than the subsidence layer.

If rain falls from the clouds building up in this layer, the heating of the air mass is hastened since the released heat will not all be consumed in the later evaporation of cloud drops. One example of heating through cumulonimbus activity is presented in fig. 3. The points on this potential temperature-mixing ratio diagram were computed from airplane psychrograph records obtained by Wyman and Woodcock in the Puerto Rico region in 1946 and reported by Bunker *et al.* (1949). The points observed inside the cloud are potentially warmer and drier than the air in the surface layer and warmer and more moist than the air which surrounds them. As this cloud mixes with the environmental air, a net warming and moistening of the cloud-layer air will result.

In the low latitudes, dry-convective turbulence ceases to be of importance in transporting heat and water vapor, since the air-sea temperature difference may drop to less than 1C. Hence, only mechanical turbulence produced at the air-sea interface and condensation convection in the cloud layer maintain the mixing process. Turbulence in the ground layer is moderate, while vertical velocities in the cumulus clouds may reach several meters per second. With the decrease in turbulence in the ground layer and the decrease in temperature gradient, the sensible heat flux drops sharply. The water-vapor flux decreases but not as markedly since the vapor gradient remains large. Using London's computations of radiational losses from the troposphere, it is estimated that the lowest levels of the atmosphere in Region 3 will lose about 60 cal cm^{-2} day^{-1}. Since this is more than the observed flow of sensible heat both from the sea and from the upper air into the layer, it is concluded that the condensation of water vapor makes up for the radiational loss. The daily heat budget for the trade winds in Region 3 is 17 cal cm^{-2} upward sensible heat, 34 cal cm^{-2} downward sensible-heat flow, 154 cal cm^{-2} upward latent-heat flow, and a loss of 60 cal cm^{-2} by radiation. A net amount of about 400 cal cm^{-2} is accumulated in a trade-wind air column during a three-day passage through the region.

The magnitude of the heat accumulated during an outburst of polar air may be estimated by summing the average values observed in the first three regions and subtracting the estimated radiation losses. If it is assumed that an air mass spends one day in each of the first three regions, 1176 cal cm^{-2} will be added to the air, and from London's work it is estimated that 120 cal cm^{-2} will be lost from the lowest levels of the atmosphere during the movement to 20N. Thus, more than 1000 cal cm^{-2} would be accumulated by the air column. Since polar air masses reach the tropics rather infrequently, their annual transport into these regions is slight. Their energies are more likely to contribute to the middle-latitude cyclones, since these air masses are usually deflected easterly or westerly before they reach the tropics. As an exporter of water vapor and sensible heat to the equatorial regions, the trade-wind system is much more important because of its greater geographical extent and constancy of flow.

REFERENCES

Budyko, M. I., 1956: Teplovoi balans zemnoi poverkhnosti. *Gidrometeorologicheskoe izdatel'stvo*, Leningrad, 255 pp. (U. S. Wea. Bur. translation, 1958: Heat balance of the earth's surface. PB131692 259 pp.)

Bunker, A. F., 1955: Turbulence and shearing stresses measured over the North Atlantic Ocean by an airplane-acceleration technique. *J. Meteor.*, **12**, 445–455.

——, 1956: Measurements of counter-gradient heat flows in the atmosphere. *Aust. J. Phys.*, **9**, 133–143.

Bunker, A. F., B. Haurwitz, J. S. Malkus, and H. Stommel, 1949: Vertical distribution of temperature and humidity over the Caribbean Sea. *Pap. Phys. Oceanogr. and Meteor.*, **11**, 1–82.

Jacobs, W. C., 1942: On the energy exchange between sea and atmosphere. *J. Mar. Res.*, **5**, 37–66.

——, 1943: Sources of atmospheric heat and moisture over the North Pacific and North Atlantic Oceans. *Ann. N. Y. Acad. Sci.*, **44**, 19–40.

——, 1951: Large-scale aspects of energy transformations over the ocean, in *Compendium Meteor.* Boston, Amer. meteor. Soc., 1057–1070.

Lettau, H. H., and B. Davidson, 1957: *Exploring the atmosphere's first mile*, Vol. 1. London, Pergamon Press, 376 pp.

London, J., 1957: *A study of the atmospheric heat balance.* Unpubl. rep. to Air Force, AFCRC–TR–57–287. Astia no. 117227.

Malkus, W. V. R., 1954: The heat transport and spectrum of thermal turbulence. *Proc. r. Soc.* A, **225**, 196–212.

Manabe, S., 1957: On the modification of airmass over the Japan Sea when the outburst of cold air predominates. *J. meteor. Soc. Jap.* Sec. II, **35**, 311–326.

——, 1958: On the estimation of energy exchange between the Japan Sea and the atmosphere during winter based upon the energy budget of both the atmosphere and the sea. *J. Meteor. Soc. Jap.* Sec. II, **36**, 123–133.

Miyazaki, M., 1949: The incoming and outgoing heat at the sea surface along the Tsushima warm current. *Ocean. Mag.* Tokyo, **1**, 103–111.

Panofsky, H. A., and R. A. McCormick, 1954: Properties of spectra of atmospheric turbulence at 100 metres. *Quart. J. r. Meteor. Soc.*, **80**, 546–564.

Priestley, C. H. B., and W. C. Swinbank, 1947: Vertical transport of heat by turbulence in the atmosphere. *Proc. r. Soc.* A, **189**, 543–561.

Priestley, C. H. B., 1954: Vertical heat transfer from impressed temperature fluctuations. *Aust. J. Phys.*, **7**, 202–209.

Riehl, H., T. C. Yeh, J. S. Malkus, and N. E. LaSeur, 1951: The north-east trade of the Pacific Ocean. *Quart. J. r. Meteor. Soc.*, **77**, 598–626.

Riehl, H., and J. S. Malkus, 1958: On the heat balance in the equatorial trough zone. *Geophysica*, **6**, 503–537.

Schmidt, W., 1921: Wird die Atmosphäre durch Konvection von der Erdoberfläche hererwärmt? *Meteor. Z.*, **38**, 262–268.

Sverdrup, H. U., 1951: Evaporation from the oceans, in *Compendium Meteor.* Boston, Am. meteor. Soc., 1071–1081.

Taylor, G. I., 1915: Eddy motion in the atmosphere. *Phil. trans. r. Soc.* A, **215**, 1–26.